

# Early Molecular Events in the Assembly of the Focal Adhesion-Stress Fiber Complex During Fibroblast Spreading

Baruch Zimmerman, Tova Volberg, and Benjamin Geiger\*

*Department of Molecular Cell Biology, The Weizmann Institute of Science, Rehovot, Israel*

Cell adhesion to the extracellular matrix triggers the formation of integrin-mediated contact and reorganization of the actin cytoskeleton. Examination of nascent adhesions, formed during early stages of fibroblast spreading, reveals a variety of forms of actin-associated matrix adhesions. These include: (1) small ( $\sim 1 \mu\text{m}$ ), dot-like, integrin-, vinculin-, paxillin-, and phosphotyrosine-rich structures, with an F-actin core, broadly distributed over the ventral surfaces of the cells; (2) integrin-, vinculin-, and paxillin-containing “doublets” interconnected by short actin bundles; (3) arrays of actin-vinculin complexes. Such structures were formed by freshly plated cells, as well as by cells recovering from latrunculin treatment. Time-lapse video microscopy of such cells, expressing GFP-actin, indicated that long actin cables are formed by an end-to-end lining-up and apparent fusion of short actin bundles. All these structures were prominent during cell spreading, and persisted for up to 30–60 min after plating. Upon longer incubation, they were gradually replaced by stress fibers, associated with focal adhesions at the cell periphery. Direct examination of paxillin and actin reorganization in live cells revealed alignment of paxillin doublets, forming long and highly dynamic actin bundles, undergoing translocation, shortening, splitting, and convergence. The mechanisms underlying the assembly and reorganization of actin-associated focal adhesions and the involvement of mechanical forces in regulating their dynamic properties are discussed. *Cell Motil. Cytoskeleton* 58: 143–159, 2004. © 2004 Wiley-Liss, Inc.

## INTRODUCTION

One of the most prominent cytoskeletal structures, present in most well-spread cultured cells, are straight bundles of actin filaments, measuring from just a few microns to tens or even hundreds of microns. These bundles, commonly denoted “stress fibers” (SF), are associated, at their termini, with focal adhesions (FA) and maintain an isometric tension, which is applied to the extracellular matrix through specialized adhesion sites [Schoenwaelder and Burridge, 1999]. The force responsible for SF-derived tension is produced by actomyosin-based contractility, which is primarily regulated by the small G-protein Rho-A [Geiger and Bershadsky, 2001].

Recent studies have indicated that SF and FA are not just physically linked, but are also highly interdependent. Thus, perturbation of the formation or maintenance of SF by inhibitors of actin polymerization or of actomyosin contractility leads to the destruction of FA [Vol-

berg et al., 1994; Tian et al., 1998; Helfman et al., 1999; Zamir et al., 1999] and inhibition of FA assembly (for example, by blocking integrin-mediated interactions) also blocks SF formation [Neff et al., 1982; Machesky

The supplemental materials referred to in this section can be found at <http://www.interscience.wiley.com/jpages/0886-1544/suppmat/index.html>

Contract grant sponsor: Minerva Foundation; Contract grant sponsor: German Israeli Foundation.

\*Correspondence to: B. Geiger, Department of Molecular Cell Biology, The Weizmann Institute of Science, Rehovot 76100, Israel. E-mail: [benny.geiger@weizmann.ac.il](mailto:benny.geiger@weizmann.ac.il)

Received 7 October 2003; Accepted 9 February 2004

Published online in Wiley InterScience ([www.interscience.wiley.com](http://www.interscience.wiley.com)).

DOI: 10.1002/cm.20005

and Hall, 1997]. Moreover, increases in cellular contractility or application of external mechanical forces induce a simultaneous growth of both FA and the attached SF [Leopoldt et al., 2001; Rivelino et al., 2001]. Interestingly, while the tight interdependence between FA and SF is obvious and supported by many lines of evidence [see: Schoenwaelder and Burridge, 1999; Burridge and Chrzanowska-Wodnicka, 1996]. The structural basis and molecular mechanisms underlying these inter-relationships are still poorly understood. Structural studies have shown that SF are highly complex structures, containing actin filaments with opposite polarities, except for the membrane-anchored ends of the cables, where the polarity is apparently uniform and the barbed ends of the filaments face the membrane [Cramer et al., 1997]. Along the bundles, there are many proteins that are involved in the contractile activity (e.g., myosin II) and its regulation (e.g., caldesmon), in actin bundling (e.g.,  $\alpha$ -actinin, filamin) or in the modulation of filament stability [Small et al., 1998]. FA too are multi-molecular complexes, containing adhesion receptors of the integrin family, different actin-binding molecules, adapter proteins, and signaling molecules [Zamir and Geiger, 2001].

Given the tight inter-dependence between mature FA and SF, one wonders what is the nature of the inter-relationships between these structures at early stages of their assembly and development? Is there a distinct "primordial complex" formed, for example, during cell spreading or migration, what are the temporal relationships between the assembly of actin bundles and establishment of early adhesions, and what is the order in which different FA molecules bind to nascent adhesion sites during spreading?

To address these issues, we have examined here early molecular events in the formation and reorganization of FA and SF during spreading of freshly plated fibroblasts or during their re-spreading following treatment with the G-actin sequestering molecule latrunculin-A (Lat-A). This treatment induces cell arborization with nearly complete loss of FA and actin bundles, yet without inducing overall cell rounding up. Following Lat-A removal, new FA-SF complexes are rapidly formed that can be visualized by antibody labeling or by dynamic recording of the reorganization of YFP-paxillin and GFP-actin in live cells. We show here that the earliest detectable forms of actin-associated adhesions are  $\sim 1\text{-}\mu\text{m}$  dots, containing integrin, vinculin, paxillin, and phosphotyrosine, with an actin core, or doublets of dots interconnected by short actin bundles.  $\alpha\text{V}\beta 3$  integrins and paxillin are consistently located at more peripheral areas of these doublets, compared to vinculin, and phosphotyrosine is widely distributed throughout the entire structure. All four labels are essentially co-localized in mature FA. Following a short phase of growth,

these doublets and the associated actin form characteristic FA-SF complexes, which tend to line up, forming extended actin bundles with integrin, vinculin, and paxillin scattered along their length. Time-lapse recording of GFP-actin in spreading cells reveals a highly dynamic reorganization of the actin cytoskeleton, manifested by fusion, shortening, convergence, and divergence of filament bundles.

## MATERIALS AND METHODS

### Cell Culture

Human foreskin fibroblasts (HFF; passages 14–28), wild type rat embryo fibroblasts (REF52), stable transfected REF52 with pBABA-YFP-paxillin-puro (prepared by Dr. Irena Lavelin and Dr. Yael Paran), and stable transfected REF52 with  $\beta 3$ -integrin-EGFP (prepared by Dr. Christoph Ballestrem at Beat A. Imhof Laboratory in Geneva as described elsewhere for GFP- $\beta 3$ -integrin-B16 cells) [Ballestrem et al., 2001] were used. All cells were maintained in culture in Dulbecco's modified Eagle's medium (DMEM), supplemented with 10% fetal calf serum, containing glutamine, penicillin, and streptomycin (Biological Industries, Kibbutz Beit Haemek, Israel). Cells were plated on glass coverslips, pre-coated with 25  $\mu\text{g}/\text{ml}$  bovine plasma fibronectin (Sigma-Aldrich Israel Ltd., Rehovot, Israel), and maintained at 37°C in a humidified atmosphere of 5%  $\text{CO}_2$  and 95% air.

### Immunochemical Reagents

Primary antibodies used in this study include: polyclonal anti-phosphotyrosine antibodies (PT40, kindly provided by Israel Pecht and Arie Licht, The Weizmann Institute) and polyclonal anti-vinculin antibodies (R694), prepared against purified chicken vinculin [Geiger, 1979]. Monoclonal antibodies against paxillin were purchased from Transduction Laboratories (Lexington, KY) and anti-vinculin (hVin1) was from Sigma-Aldrich Israel Ltd. (Rehovot, Israel). Cy3-conjugated goat anti-mouse F(ab')<sub>2</sub> fragments were purchased from Jackson ImmunoResearch Laboratories (West Grove, PA). Alexa 488-conjugated goat anti-rabbit IgG (H+L) was purchased from Molecular Probes (Eugene, OR). FITC-labeled phalloidin was purchased from Sigma-Aldrich Israel Ltd.

### Immunofluorescence Staining

The cells were simultaneously permeabilized and fixed for 2 min with 0.5% Triton X-100 (Sigma-Aldrich Israel Ltd), 3% paraformaldehyde (Merck, Darmstadt, Germany) in phosphate-buffered saline (PBS), and then post-fixed with 3% paraformaldehyde for an additional

30 min. The cells were washed with PBS, double-labeled with the primary (mouse and rabbit) antibodies for 30 min, washed in PBS, and further incubated for 30 min with Cy3-conjugated goat anti-mouse and either Alexa 488-conjugated goat anti-rabbit antibodies or FITC-labeled phalloidin. The samples were washed again with PBS and mounted on slides, using Elvanol (Mowiol 4-88, Serafon, Ashdod, Israel).

### Latrunculin A-Induced Disruption of the Actin Cytoskeleton

REF52 cells were plated on fibronectin pre-coated coverslips and incubated at 37°C for 24 h. The cells were then treated with 1  $\mu$ M Latrunculin A (Molecular Probes) for 5 h. The drug was then washed with fresh medium and the cells were further incubated at 37°C for different time points, as indicated.

### Expression of YFP-Actin in REF52 Cells

To visualize actin filaments in live cells, REF52 cells were transfected with a vector, encoding YFP-Actin fusion protein (prepared by Dr. Joachim Kirchner). Actin cDNA (from *Dictyostelium*) was ligated in frame into the EcoR1 site of the EYFP-C2 plasmid (Clontech, Palo Alto, CA). REF52 cells were transfected with this plasmid. Sub-confluent cells were suspended in electroporation buffer (20 mM HEPES, 137 mM NaCl, 5 mM KCl, 0.7 mM Na<sub>2</sub>HPO<sub>4</sub>, 6 mM dextrose, and 1 mg/ml BSA, adjusted to pH 7.05, mixed with the YFP-actin vector (60  $\mu$ g), and electroporated using a GENE PULSER II system (Bio-Rad, Hercules, CA). After the electroporation, the cells were collected by centrifugation, resuspended in DMEM, and plated on glass-bottom microwell dishes (MatTek, Ashland, MA).

### Digital Immunofluorescence Microscopy

Quantitative fluorescence microscopy was carried out using the DeltaVision system (Applied Precision, Issaquah, WA) using an inverted Zeiss Axiovert microscope with a 100 $\times$ /1.3 PlanNeofluoar objective (Zeiss, Oberkochen, Germany). Images were processed using the Priism software of the DeltaVision system as previously described [Zamir et al., 1999]. The processing employed here included the following routines:

1. Image filtration: original images of immunostained cells were subjected to high-pass filtration subtracting the local average intensity surrounding each matrix adhesion site.
2. "Spectral" presentation of fluorescence intensity: fluorescence intensities of filtered images were presented using a blue-to-red linear spectrum color scale.

3. Fluorescence ratio imaging (FRI): cells were double-labeled for pairs of proteins, the images were subjected to filtration and the intensity ratio was computed per pixel as previously described [Zamir et al., 1999]. The ratio images are presented in a logarithmic spectrum scale.

### Time-Lapse Recording

YFP-paxillin stably transfected and YFP-actin, transiently transfected REF52 cells were plated on glass-bottom microwell dishes, and maintained at 37°C on the microscope stage in medium, buffered with 10 mM HEPES, pH 7.0, and kept at 37°C. Images were acquired using the DeltaVision system. Paxillin movie was taken with 1-min intervals, starting immediately after removal of Lat-A. The intervals between images in the actin movie were 1 min at the first 50 min after Lat-A removal and 3–5 min upon longer incubation. For convenient visual evaluation of the displacement of the labeled actin, sequential red-green pairs of images were superimposed so that the green represents the "later" localization of the protein and the red represent the "earlier" one.

### Scanning Electron Microscopy

REF52 cells, plated on glass coverslips, were treated with Lat-A and allowed to recover as indicated. The cells were then fixed for 1 h with 2% glutaraldehyde and 3% paraformaldehyde in 0.1 M cacodylate buffer containing 5 mM CaCl<sub>2</sub> and 1% sucrose, pH 7.2. The cells were rinsed three times, 3 min each, with 0.1 M cacodylate buffer and post-fixed for 1 h with 1% osmium tetroxide in the same buffer and rinsed with cacodylate buffer followed by water. The coverslips were then treated with 1% tannic acid for 5 min followed by 30 min with 1% Uranyl acetate (in water). The coverslips were then rinsed again, dehydrated in ethanol, and critical point dried (Pelco CPD2, Ted Pella, Redding, CA). The samples were sputter-coated with gold for 6 min at 10 mA, followed by 6 min at 20 mA (S150 Edwards, Sussex, UK) and examined in a JSM-6400 scanning electron microscope (JEOL, Tokyo, Japan) operated at 20 kV.

## RESULTS

### Formation of Early Matrix Adhesions During Fibroblast Spreading

Within 2–3 min after plating of HFF cells on fibronectin-coated coverslips, cell attachment was apparent, followed, within 1–2 min later, by an initial spreading on the surface. Fixation of cells, 5 min after plating, and labeling for vinculin (Fig. 1, raw image, 5min) revealed extensive labeling around the cell center, with small faint patches at the periphery. 3D deconvolution of

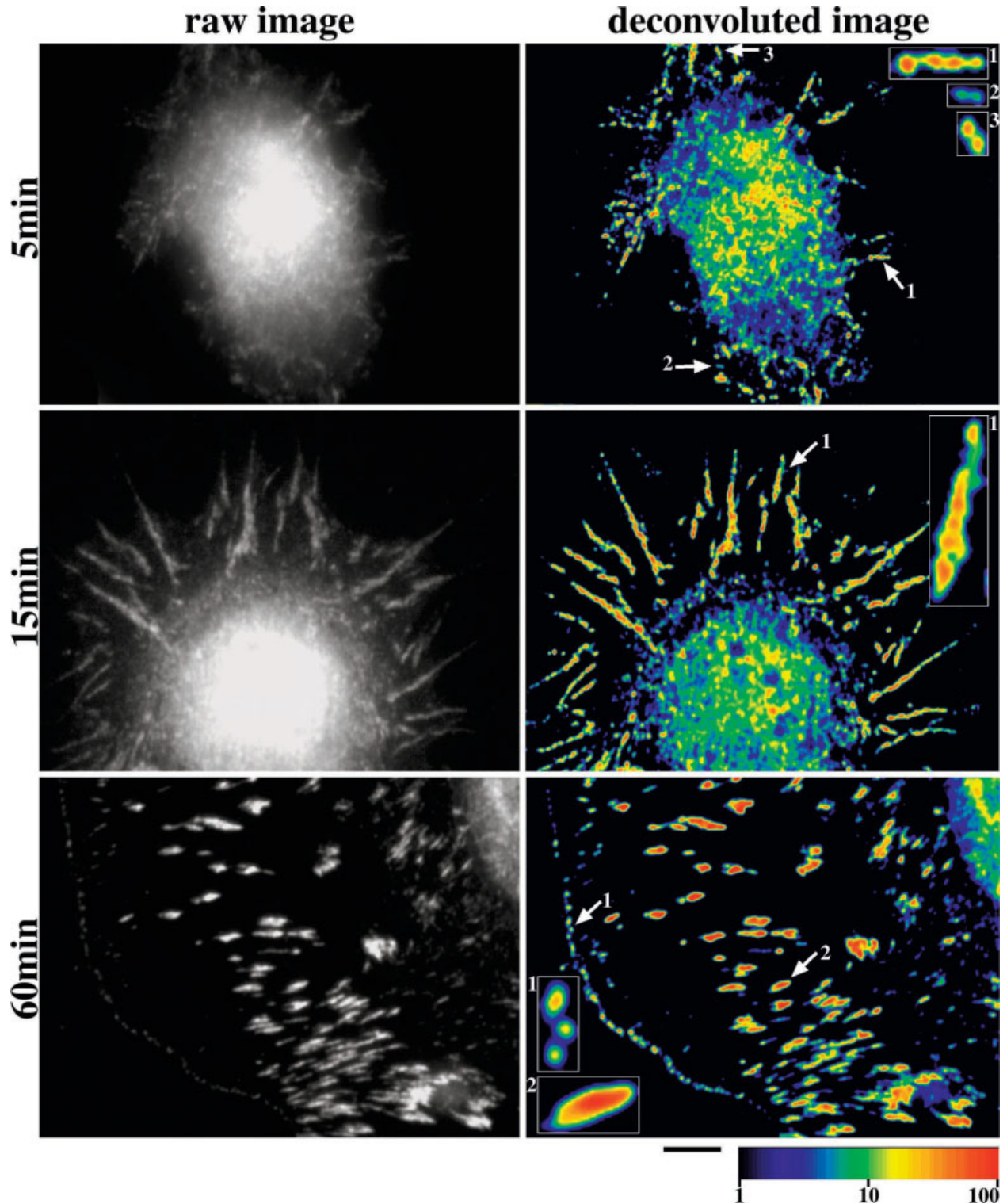


Fig. 1. Formation of early matrix adhesions during cell spreading. Human foreskin fibroblast cells were plated on glass coverslips, fixed 5, 15, or 60 min later, and labeled for vinculin. **Left:** The raw immunofluorescent images. **Right:** The corresponding images following 3D deconvolution. At 5 min after plating, vinculin is associated with small dot-like adhesions, often arranged in doublets or short

chains. After 15 min, the vinculin dots become more ordered, forming long radial chains. At 60 min after plating, vinculin is already associated with typical elongated mature focal adhesions as well as in peripheral dots resembling focal complexes. The right column is presented with a spectrum intensity scale. Bar = 5  $\mu$ m.

focal stacks of such images revealed numerous vinculin-rich dots along the cell-matrix interface (Fig. 1, deconvoluted image, 5min). These dots had an apparent diameter in the range of 0.5–1  $\mu\text{m}$ , and they were usually clustered into pairs or small radial arrays (Fig. 1, 5min, insets). Within 15 min after plating, spreading became considerably more prominent and the arrays of dots became larger and denser, though individual dots or dot doublets could still be discerned (Fig. 1, deconvoluted image, 15 min). By 60 min, two major forms of vinculin-rich adhesions were detected in the cells, namely peripheral focal complexes, with a typical appearance of small, single dots, located close to the leading edge of the cell, and more centrally located FA (Fig. 1, 60min). Attempts to monitor, in parallel, actin assembly in spreading cells, did not yield images of sufficient resolution, and for that purpose we have used cells, re-spreading after latrunculin-treatment (see below).

### Formation of Early Matrix Adhesions Following Latrunculin-A Treatment

Incubation of well-spread REF52 cells with 1  $\mu\text{M}$  Latrunculin-A (Lat-A) resulted in an overall cell arborization, creating numerous, substrate-attached highly branched thin cellular extensions (typically  $\sim 1\text{--}1.5$   $\mu\text{m}$  in diameter). Scanning electron microscopy often revealed a characteristic “pearling pattern” along these processes (Fig. 2, compare a and b panels) similar to those described by Bar-Ziv et al. [1999]. Upon withdrawal of Lat-A, rapid re-spreading occurred, leading to flattening of the cell body and transformation of the peripheral branches into extended flat regions at the cell periphery. These changes were prominent already within 5–15 min after removal of Lat-A, and acquisition of flat morphology was nearly complete between 30 min and 2 h (Fig. 2).

Since re-spreading after latrunculin withdrawal occurs while the cell periphery remains rather flat, and suitable for high-resolution light microscopy, we have investigated in detail the early stages in FA-SF assembly in this system. As shown in Figure 3, the most prominent residual adhesion structures found in the Lat-A treated cells, which formed immediately after Lat-A removal, are small vinculin-rich dots and dot-doublets (Fig. 3a and b). The typical diameter of the single dots was  $\sim 1$   $\mu\text{m}$  and the vinculin labeling intensity was particularly enriched at the periphery of this structure, with lower intensity in the center. Double labeling of the same cells for actin revealed a reciprocal intensity gradient, namely an enrichment of actin labeling in the core of the dot, and reduced level at the periphery (see ratio image in Fig. 3). Examination of early adhesions in many cells indicated that the vinculin “rings” could often be incomplete (see, for example, the vinculin panels in Figs. 3a and 4a) and

apparently split into vinculin doublets. The notion that the initial vinculin dot develops into a doublet is corroborated by the fact that distinct doublets were increasingly prominent following incubation for 5–15 min after Lat-A removal, and that unlike the initial dot, each of the paired dots forming the doublet had a vinculin-rich core. Labeling for actin revealed a small bundle interconnecting the paired dots (Fig. 3b).

Upon a longer recovery period (usually 10–20 min), such doublets tend to either grow or be replaced by large FA-SF-like complexes, 5–10  $\mu\text{m}$  long, as shown in Figure 3c (arrow). In some cases, such doublets appear to line up, forming long actin cables with vinculin associated with their termini as well as along their length (Fig. 3d, arrow). This apparent end-to-end lining-up of FA-SF complexes continues and by 15–30 min after Lat-A withdrawal, large bundles with vinculin patches scattered along their length are found.

### Differential Distribution of Vinculin, $\alpha\text{V}\beta 3$ Integrin, Paxillin, and PY in Newly Formed Matrix Adhesions

To characterize the molecular organization of early matrix adhesions, we have compared the localization of vinculin to that of  $\alpha\text{V}\beta 3$  integrin, paxillin, and PY in cells, at different stages of re-spreading following Lat-A treatment. Labeling for vinculin in conjunction with  $\alpha\text{V}\beta 3$  (using  $\beta 3$ -GFP-expressing cells) or with paxillin revealed extensive but incomplete overlap. Thus,  $\alpha\text{V}\beta 3$  and paxillin were consistently located more peripherally in the early dots and small doublets (Figs. 4 and 5a). These relationships were maintained also in the large FA-SF complexes (Figs. 4 and 5b). During later stages of assembly, when end-to-end alignment of the doublets and formation of long bundles were apparent, the distribution of all these FA proteins was similar, with only small local variations (Figs. 4 and 5c–e).

PY, which is largely co-localized with paxillin and vinculin in FA [Zamir et al., 1999], was broadly distributed throughout the initial dots and doublets, including their central cores, where actin was particularly prominent (Figs. 6a,b and 7a,b). At later stages of assembly, PY was mainly restricted to the vinculin- and paxillin-rich FA (Figs. 6c–e and 7c–e).

### Dynamic Analysis of FA and Stress Fibers Assembly and Reorganization

The sequence of events involved in FA-SF assembly, proposed above, is indirectly supported by observations made with cells, fixed at different time points and, relating the “static” structural features to specific stages in the dynamic process of FA-SF assembly. To obtain direct information on the assembly of these structures, REF52 cells expressing YFP-actin and YFP-paxillin

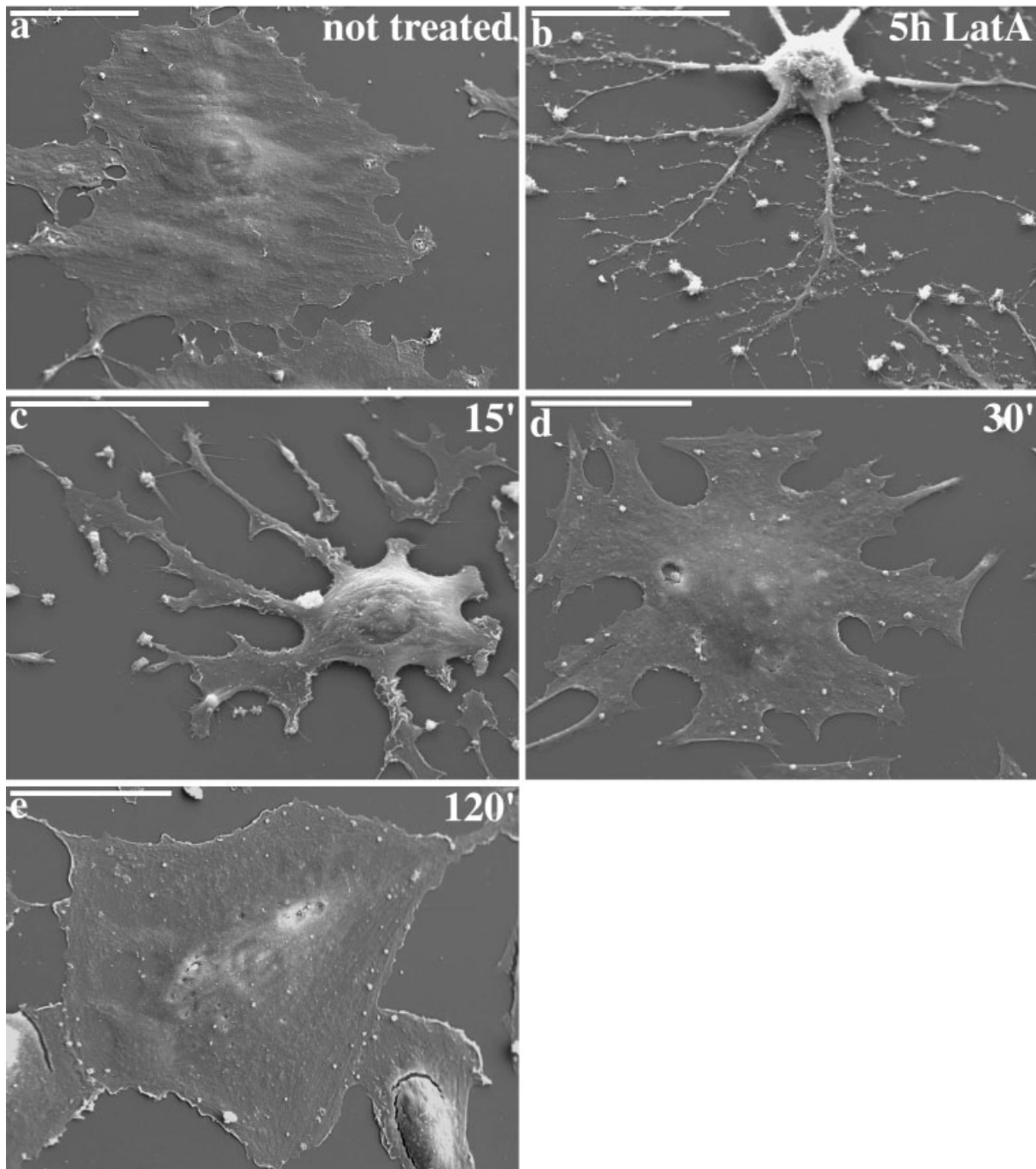


Fig. 2. Scanning electron micrograph showing re-spreading of REF52 cells following latrunculin-A (Lat-A) treatment and withdrawal. **a:** Untreated cells; **b:** Cells treated for 5 h with 1  $\mu\text{g/ml}$  Lat-A. **c–e:** Lat-A treated cells (as in b), incubated in normal medium for 15, 30, or 120 min. Note the arborization and rounding up of the cell after treatment and the time-dependent re-spreading and acquisition of normal, flat morphology after Lat-A removal. Bar = 50  $\mu\text{m}$ .

were monitored by time-lapse video microscopy during Lat-A treatment and recovery.

Figure 8 demonstrates the dynamic evolution of a long FA-SF complex, originating in small, distinct dou-

blet structures. Frames were taken from a time-lapse movie of YFP-paxillin expressing cells, during re-spreading after Lat-A treatment. Figure 8 (top left) shows, in a spectrum intensity scale, the cell's paxillin

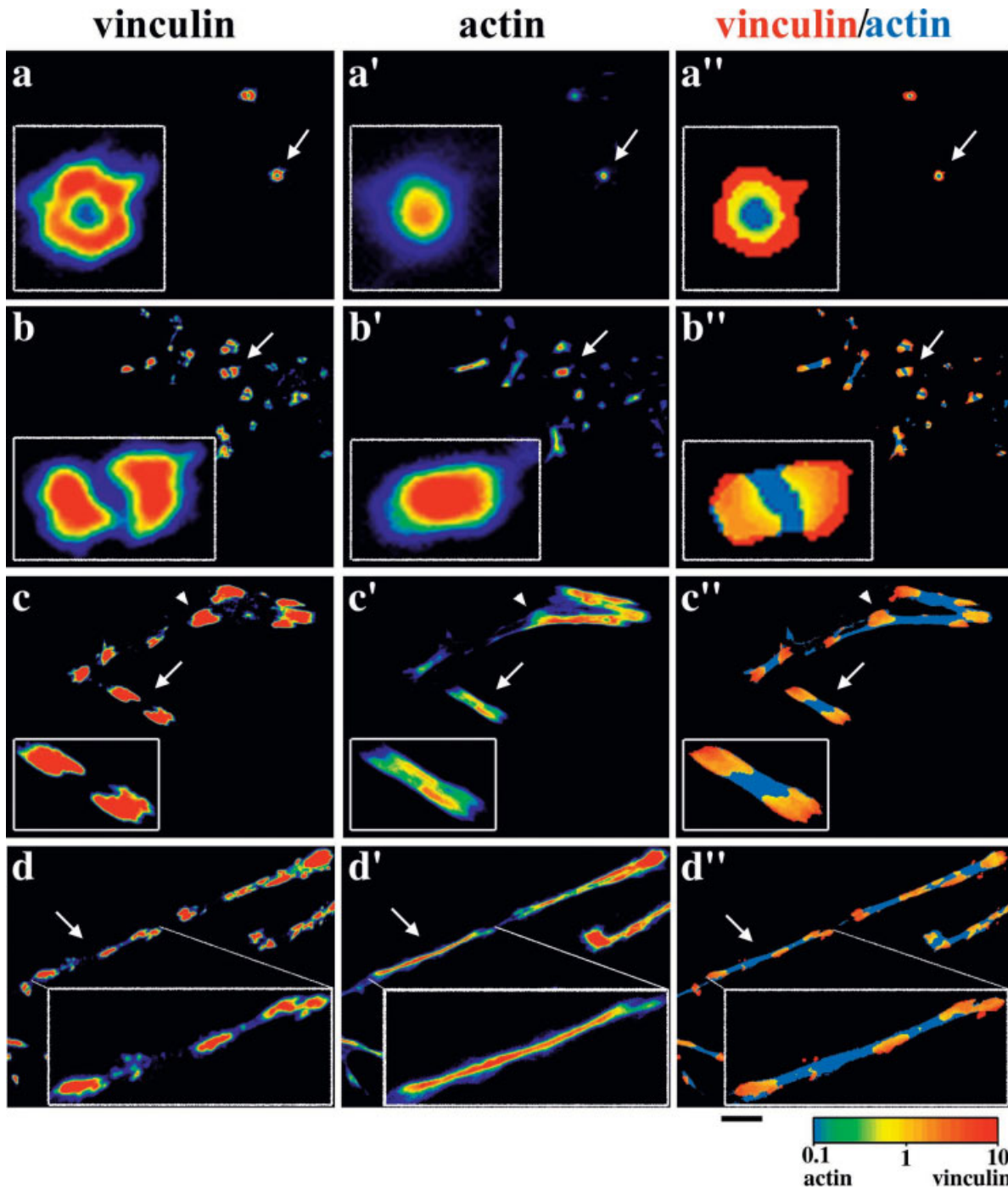


Fig. 3. Initial stages in the formation of actin- and vinculin-associated adhesions during the re-spreading of REF52 cells, following Lat-A withdrawal. Cells were treated with Lat-A for 5 h, fixed within 5 min after removal of the drug, and double-labeled for vinculin (left) and F-actin (center). The intensity of the two proteins is presented in a blue-to-red spectrum scale. Right: The fluorescence ratio images in a spectrum scale representing the ratio value. Arrows point to structures magnified in the insets. Four major forms of actin and vinculin

organization observed following short recovery are presented in rows a–d. **Rows a:** The smallest detectable adhesions consist of vinculin dot or ring structures (typical diameter of 1  $\mu\text{m}$ ) with an actin core; **b:** separated vinculin-rich dot-doublers interconnected by a short F-actin bundle; **c:** elongated and enlarged vinculin doublers (typical size of 5–10  $\mu\text{m}$ ), interconnected by a large actin bundle; **d:** Long chains of vinculin-rich structures (e.g., doublers), connected by a long actin bundle. Bar = 5  $\mu\text{m}$ .

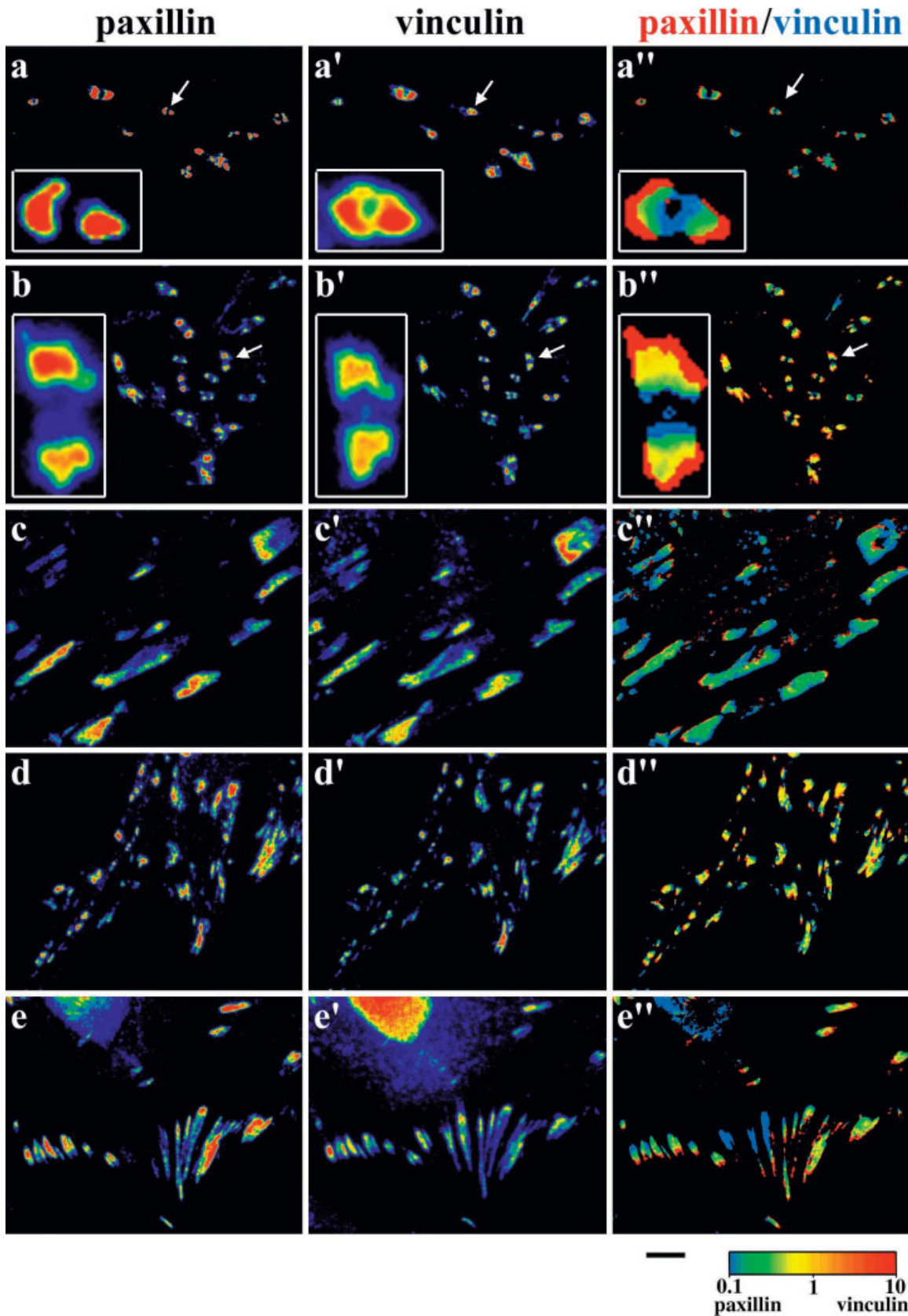


Fig. 4. Differential distribution of paxillin and vinculin in matrix adhesions of spreading cells. REF52 fibroblasts were treated with Lat-A and allowed to recover for different time periods and double labeled for paxillin and vinculin, Images are presented as described in the legend to Figure 3. Arrows point to structures magnified in the insets. Early stages in re-spreading (rows **a,b**) were recorded just

before and within 5 min after Lat-A withdrawal, intermediate stages (rows **c,d**) after 10 and 30 min, and well-organized focal adhesions after 2 h or more (row **e**). Notice the differential distribution of the two proteins, indicating that paxillin is localized in more peripheral areas than vinculin. These differences are most conspicuous in the ratio images of small doublets. Bar = 5  $\mu$ m.

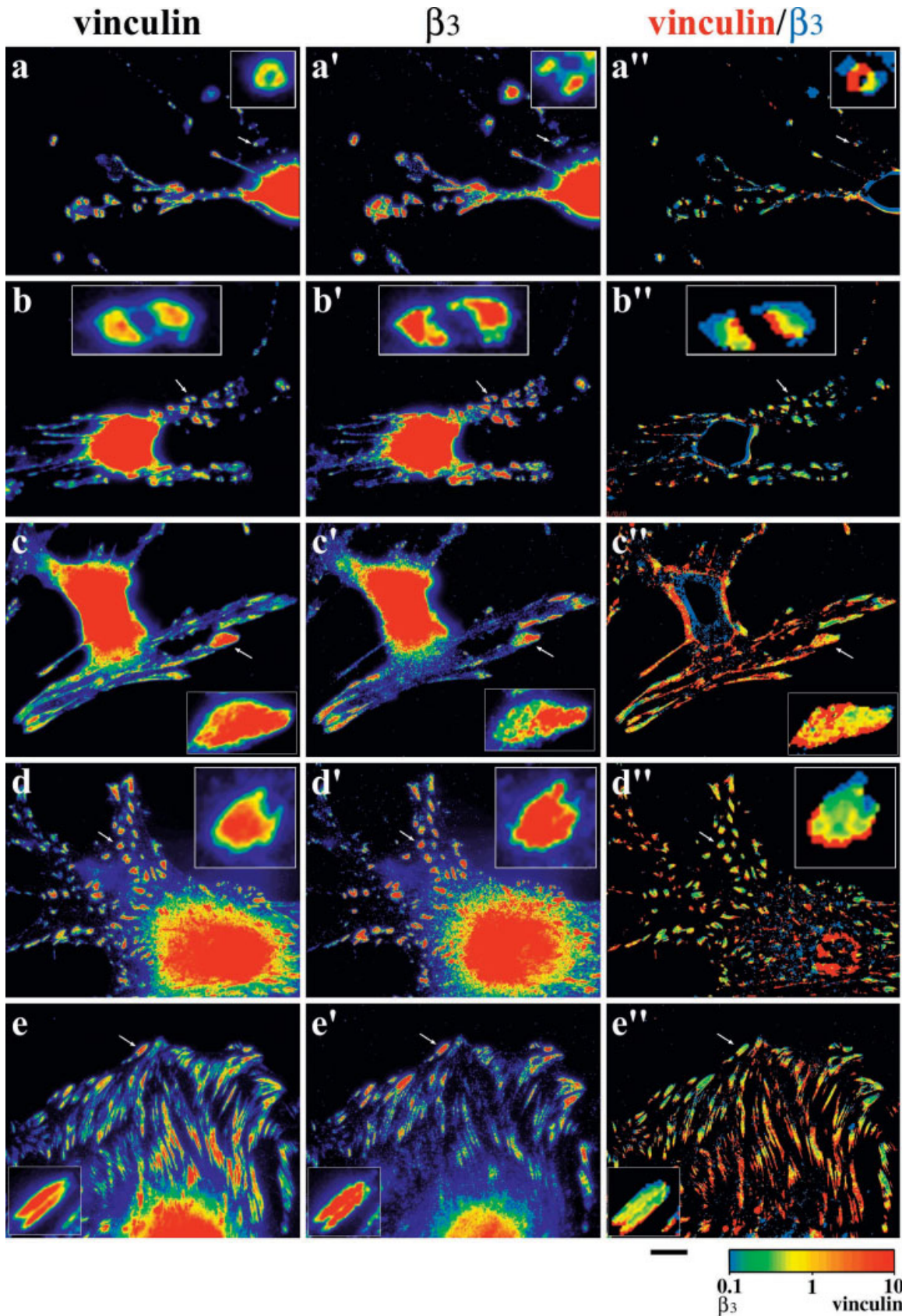


Fig. 5. Differential distribution of  $\alpha V\beta 3$  integrin and vinculin in matrix adhesions of spreading cells. REF52 fibroblasts, stably expressing GFP- $\alpha V\beta 3$ , were treated with Lat-A, allowed to recover for different time periods, and double labeled for GFP and vinculin. Images are presented as described in the legend to Figure 3. Arrows point to structures magnified in the insets. Early stages in re-spreading (rows **a,b**) were recorded just

before and within 5 min after Lat-A withdrawal, intermediate stages (rows **c,d**) after 10 and 30 min, and well-organized focal adhesions after 2 h or more (row **e**). Notice the differential distribution of the two proteins, indicating that  $\alpha V\beta 3$  is localized in more peripheral areas than vinculin. These differences are most conspicuous in the ratio images of the small doublets. Bar = 5  $\mu\text{m}$ .

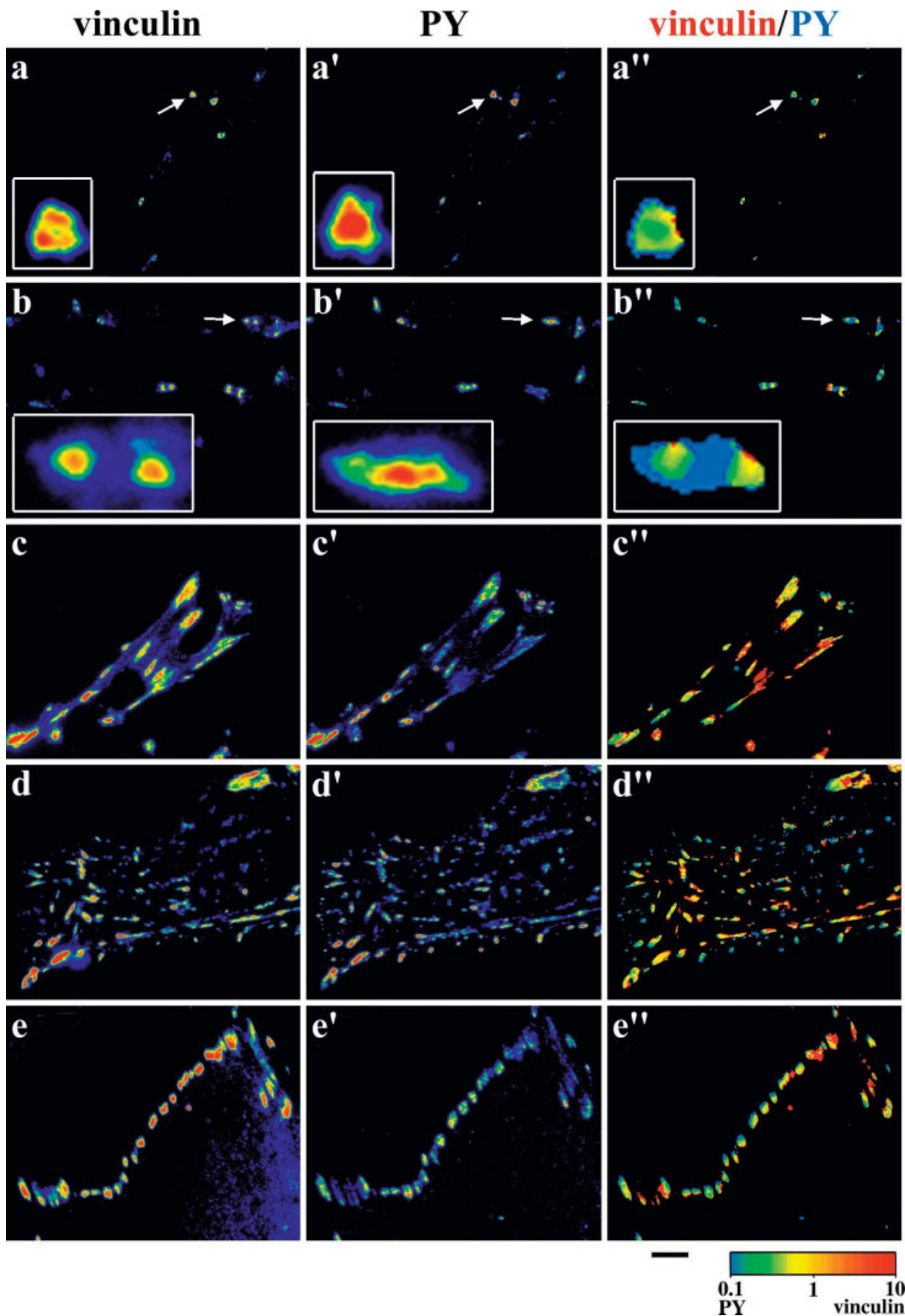


Fig. 6. Differential distribution of vinculin and phosphotyrosine (PY) in matrix adhesions of re-spreading cells. REF52 fibroblasts were treated with Lat-A and allowed to recover for different time periods and double labeled for phosphotyrosine and vinculin, Images are presented as described in the legend to Figure 3. Arrows point to structures magnified in the insets. Early stages in re-spreading (rows **a,b**) were recorded just before and within 5 min after Lat-A with-

drawal, intermediate stages (rows **c,d**) after 10 and 30 min, and well-organized focal adhesions after 2 h or more (row **e**). Notice the differential distribution of vinculin and phosphotyrosine, manifested by widespread phosphotyrosine localization throughout the plaque (often extending beyond vinculin) as well as in more central areas. These differences are most conspicuous in the ratio images of small doublets. Bar = 5  $\mu$ m.

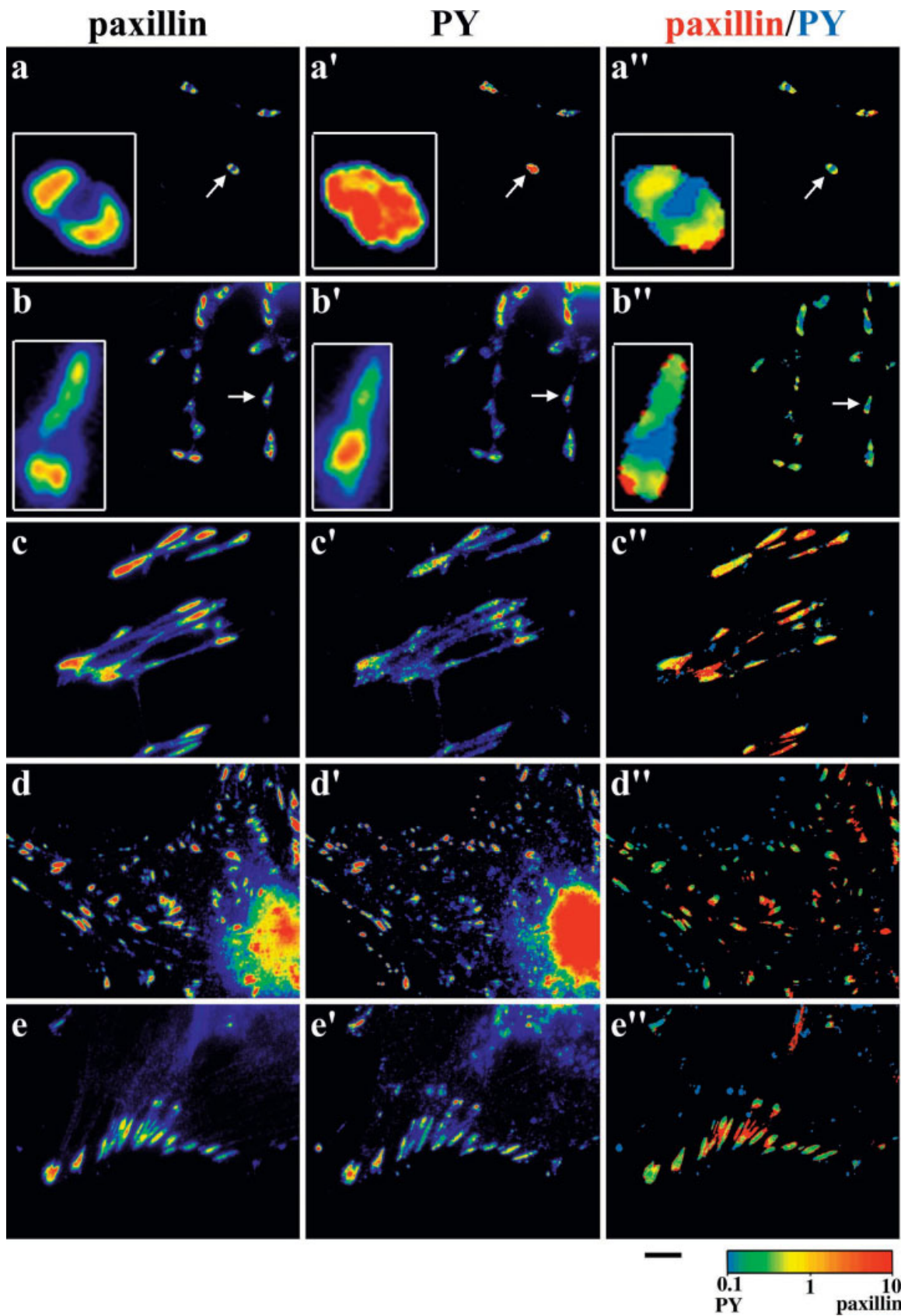


Fig. 7. Differential distribution of paxillin and phosphotyrosine (PY) in matrix adhesions of spreading cells. REF52 fibroblasts were treated as and double labeled for phosphotyrosine and vinculin as described for Figure 3. Arrows point to structures magnified in the insets. Early stages in re-spreading (rows **a,b**) were recorded just before and within

5 min after Lat-A withdrawal, intermediate stages (rows **c,d**) after 10 and 30 min, and well-organized focal adhesions after 2 h or more (row **e**). Notice the widespread distribution of phosphotyrosine localization throughout the paxillin-rich plaque and in more central areas. Bar = 5  $\mu$ m.

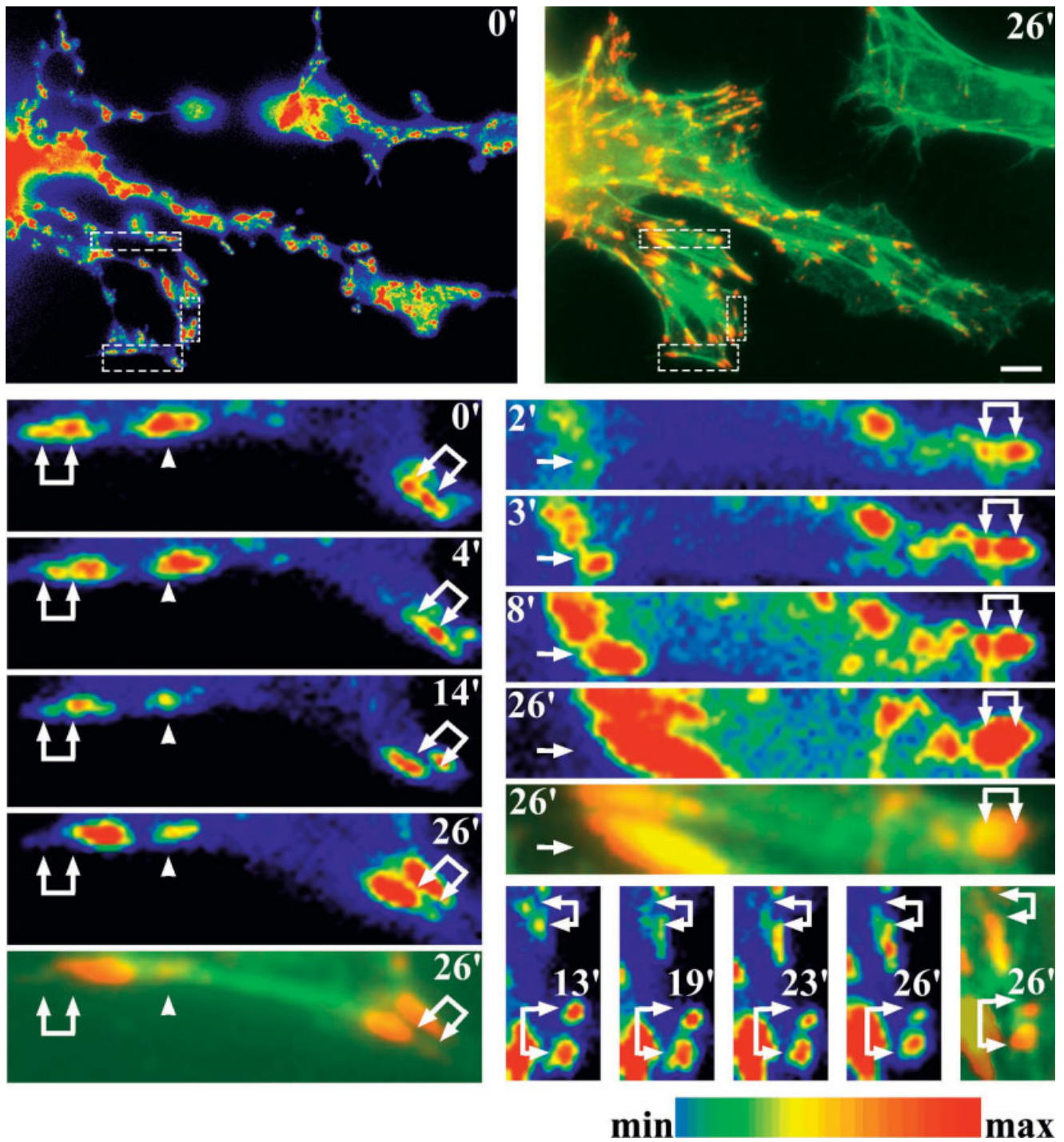


Fig. 8. Alignment of FA doublets and formation of mature FA-SF complexes as revealed by time-lapse video microscopy of YFP-paxillin. REF52 cell line, stably expressing YFP-paxillin, was treated with Lat-A and the re-spreading was monitored. **Top left:** Paxillin distribution after Lat-A treatment (intensity, spectrum scale presentation). **Top right:** Distribution of paxillin and actin (by phalloidin staining)

26 min after removing the drug. **Lower panels:** Individual frames taken from the movie. *Arrows* and *arrowheads* indicate the initial position of paxillin doublets. Notice that as re-spreading progresses, doublets line up and inner doublets (arrowhead) fade away while FA located at the ends of the actin cables grow. Double arrows indicate a doublet structure. Bar = 2  $\mu$ m

distribution after Lat-A treatment. Figure 8 (top right) shows (in green/red superposition) the actin/paxillin distribution 26 min after withdrawal of the drug. The sequence of images on the left shows the alignment of three individual doublet structures (arrows and arrowhead) (time point 0'). Upon FA development, the outer doublets (arrows) are losing their "inner" paxillin dots while the "outer" dots grow. At the same time, doublets located along the actin bundle (arrowhead) are fading away. The result of that process, as shown at the latest time point (26'), is the assembly of a long SF, anchored at both ends to mature FA. The images on the right show two additional examples from the same cell for a similar alignment of doublets and formation of SF.

Several key steps in the formation of F-actin-containing bundles are shown in Figure 9. For the sake of clarity, we present here selected pairs of frames from a time-lapse movie, where two sequential time points are shown in red (earlier) and green (later). Overlapping areas are shown in yellow. Examination of such images, frame by frame, reveals a variety of actin-rich structures, including stationary bundles (e.g. #2 in the 0'/1' frame, Fig. 9), and highly mobile, spherical structures (e.g. #1 in the 0'/1' frame of Fig. 9). Both structures can develop into short bundles of F-actin via an apparently similar mechanism, namely a rapid "sprouting" process. This transformation occurs, for example, between 5'-7' after Lat-A removal for structure #2, and between time points 26'-27' for #1 (Fig. 9). For dynamic visualization, see supplement Movies 2 and 3.

Subsequent stages in SF assembly, namely, end-to-end fusion of short bundles, leading to the formation of long SF, are also apparent from Figure 9 and shown in greater detail in Figure 10 (see, for example, the merger of 2 fibers at time points 31' and 43' in Fig. 10) and the subsequent merger of the fused bundle with another SF (between 80'-116') forming a long SF. The fusion of two bundles into one is accompanied by alignment of the two along one axis, which is often different from the original orientation of the two "mother fibers." For dynamic visualization, see supplement Movie 4. Evidently, this process of SF fusion, divergence, and lateral shift is a characteristic feature of SF dynamics in general, not restricted to Lat-A treatment or recovery (B. Zimerman, data not shown).

## DISCUSSION

In the present study, we have addressed the dynamic processes underlying the assembly of new FA-SF complexes in spreading cultured cells. This process, which is crucial for both cell adhesion and assembly of the actin cytoskeleton, presents an intriguing apparent paradox related to the involvement of mechanical force in cell adhesion and cytoskeleton organization. Though

the formation of FA is essential for the assembly of the contractile, actomyosin-based system, FA development also strictly depends on the contractility of the very same actomyosin network [Geiger and Bershadsky, 2002]. How then are the very first SF-FA complexes formed at the onset of cell-matrix interaction before contractile bundles assemble?

Our approach to this dilemma was to directly examine the structural and molecular properties of the earliest-detectable matrix adhesions, formed shortly after the establishment of matrix contacts. We employed here two experimental systems, namely, fibroblasts, freshly plated on fibronectin-coated surfaces, and cells undergoing re-spreading on the substrate following treatment with the G-actin-sequestering macrolide, latrunculin. Both systems revealed largely similar, dot-like adhesions, formed shortly after plating, or Lat-A withdrawal. However, the latrunculin-treated cells had some advantages in as much as they enabled better visualization of small and rather faint adhesion- and cytoskeleton-associated structures. Lat-A was selected for these studies since it binds to and sequesters monomeric actin, and does not directly interact with or modify actin filaments or filament bundles [Ayscough, 1998].

The assembly of focal adhesions and actin bundles was recorded here primarily by labeling cells at different time points after plating or after Lat-A withdrawal from the culture medium, for actin and a variety of focal adhesion molecules. Monitoring of these processes in live cells expressing GFP derivatives of the corresponding molecules was successful only for visualization of rather advanced stages in FA-SF assembly, since small, newly formed adhesions were too faint to be resolved in live cells, and both over-expression of the proteins or excessive illumination affected the development of new cytoskeleton-bound adhesions and were thus avoided.

We have used both direct, dynamic data, based on live cell recording, and fluorescent labeling of cells fixed at specific stages in FA and SF assembly. Examination of the adhesion sites formed during the first few minutes after plating (recognized by their vinculin labeling and localization at the focal plane of the substrate) revealed different stages in the assembly of these structures, included: (1) Dot-like adhesions, measuring  $\sim 1 \mu\text{m}$  in diameter, which contain an actin core and an integrin-vinculin- and paxillin-rich periphery. Phosphotyrosine was abundant throughout these structures. These dots resemble classical podosomes [Geiger and Bershadsky, 2001; Linder and Aepfelbacher, 2003] and are apparently short lived since they can be detected only during the first few minutes of spreading. (2) Integrin-vinculin-paxillin-containing "doublets" of adhesion sites, interconnected by actin. The origin of these small complexes is not directly defined here though we suggest that they are

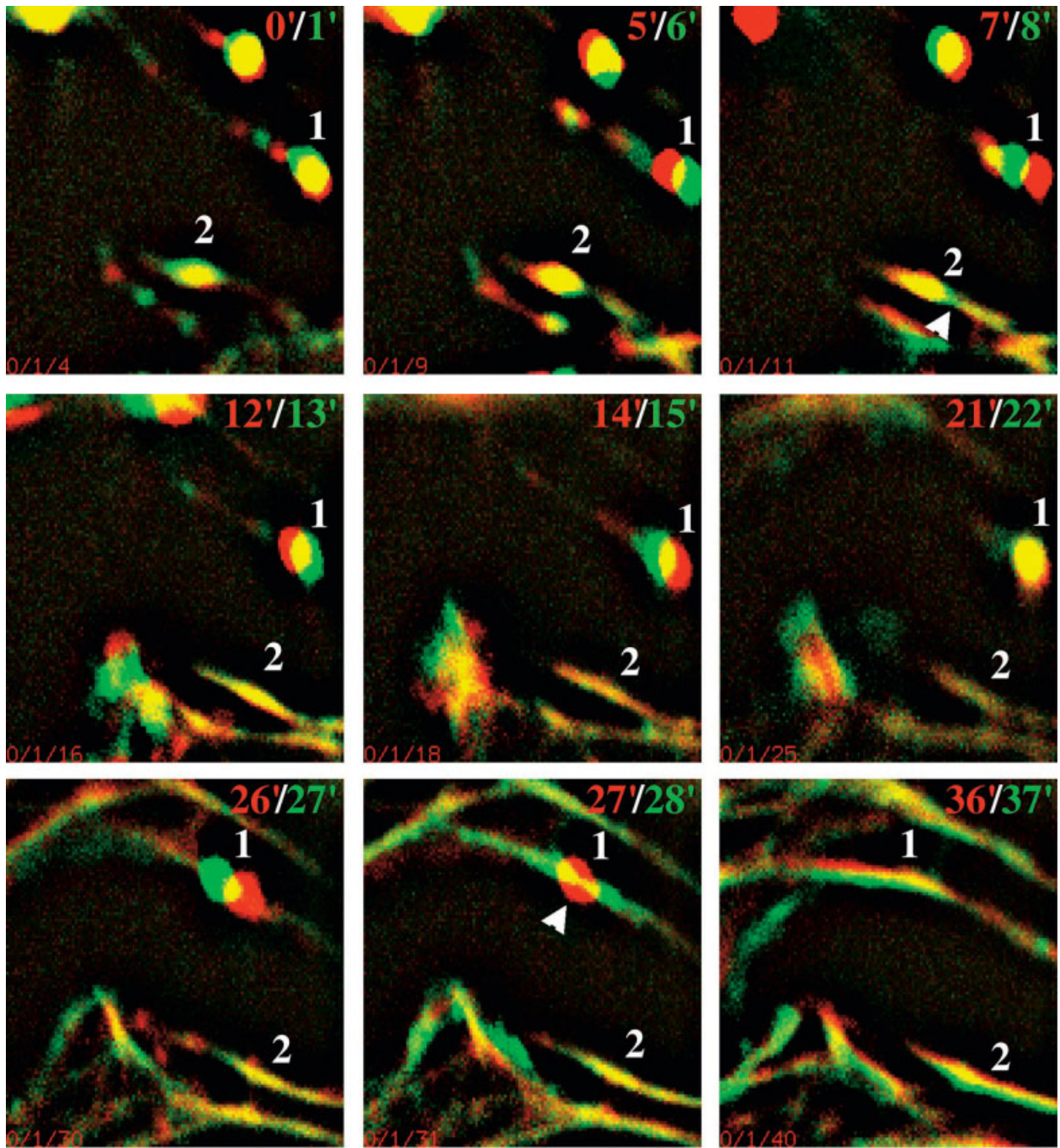


Fig. 9. Formation and reorganization of actin bundles during early stages of spreading of REF52 cells, as revealed by time-lapse video microscopy of GFP-actin. At early stages of recovery from Lat-A treatment, actin-rich spherical foci (marked 1 and 2) move along cell arborizations, elongate and develop into actin bundles. In this temporal presentation taken from a time-lapse movie, *green* represents the

“present” localization of actin, while *red* represents the “former” localization (1-min shift). *Arrowhead* highlights the point of “sprouting” of actin filaments from the spherical foci. Numbers in the top right corners indicate time in minutes after removal of Lat-A. Bar = 5  $\mu$ m. See supplementary Movie 3.

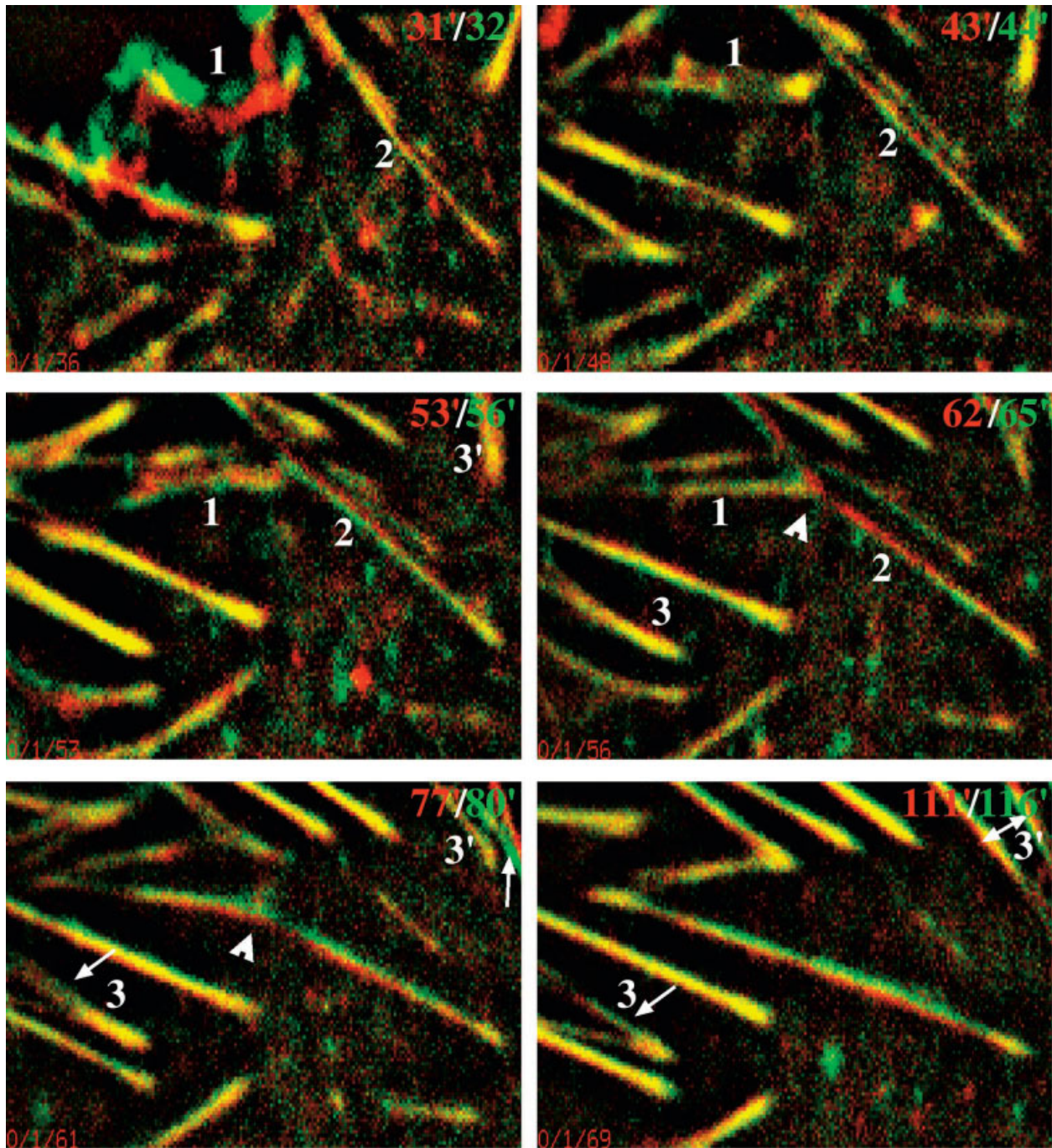


Fig. 10. Different modes of dynamic rearrangement of actin filaments in live REF52 cells. *Green-red* superimposed images depict the changes in actin organization as described in the legend to Figure 7. Actin bundles (marked 1 and 2) often translocate laterally, align end to end, and fuse into one continuous bundle (*arrowheads* point the place of fusion). Other filaments (marked 3 and 3') apparently split or diverge (*arrow*). Numbers in the top right corners indicate time in minutes after removal of Lat-A. Bar = 5  $\mu$ m. See supplementary Movie 4.

derived from the dots described above. The possibility that the dots actually “split” into these doublets is indirectly corroborated by the fact that these two structures

have largely similar dimensions, and that intermediate forms displaying “partial splits” (see, for example, Fig. 3) can frequently be detected. (3) FA-SF complexes (4–6

$\mu\text{m}$  long) consisting of two definitive focal adhesions interconnected by a robust actin bundle. (4) Chains of such FA-SF complexes forming extended stress fiber-like structures. It should be noted that, unlike “mature” SF of well-spread cells, the bundles formed during spreading contained vinculin and paxillin patched not only at the ends but also along the entire length of the actin filaments.

It is noteworthy that the early adhesions described above contained  $\alpha\text{V}\beta\text{3}$  integrin, vinculin, and paxillin, and were tyrosine phosphorylated, yet the distributions of the four labels were not entirely overlapping (Figs. 4–7). Some differential distribution of vinculin and paxillin is occasionally observed along the margins of mature focal adhesions, yet phosphotyrosine labeling in mature adhesions is usually strictly co-localized with paxillin (Zimerman and Geiger, unpublished observation).

The process outlined above appears to be quite general, and similar intermediate stages in SF and FA formation were resolved during spreading of several cell types, including Pig Aortic Endothelial Cells and 3T3 fibroblasts. It is, however, different from the “classic” assembly of these structures in well-spread cells during cell locomotion. It has been demonstrated that the extension of lamellipodia by motile cells is accompanied by the formation of numerous dot-like adhesions under the leading edge, known as “focal complexes.” [Nobes and Hall, 1995]. The formation of these structures is stimulated by the small G-protein Rac-1 and upon application of contractile forces, some of these adhesions transform into bona fide focal adhesions [Rottner et al., 1999]. The formation of FA during early cell spreading is different in many ways; it takes place at different sites along the ventral cell surface (Fig 1), and it develops through characteristic “doublet” structures that grow, line up, and fuse, eventually forming long bundles (Fig. 3).

Time-lapse monitoring of the reorganization of actin and paxillin in the spreading cells directly confirmed the modular re-assembly of the FA and the associated micro-filament system. This includes the formation of paxillin doublets, their alignment and development into mature FA. Careful examination of actin dynamics in the spreading cells showed that short actin bundles (typically  $2\ \mu\text{m}$  in length) were formed within minutes after Lat-A removal, apparently emerging from actin-rich foci (see, for example Fig. 9, and also Supplementary Movie 2 and 3). Similar actin filaments were also found in freshly plated cells, though their structural details and origin could not be readily resolved (data not shown). Following a fast initial growth (typically, within 0.5–1 min), these filaments reach a length in the range of 3–4  $\mu\text{m}$  and apparently stop elongating. These filament bundles often fuse, end-to-end, and form relatively long bundles. Further monitoring of this filament network revealed a progressive rearrangement of the filaments, manifested by shortening, splitting, converg-

ing, or lateral shifting (see Fig. 10 and also Supplementary Movie 4, starting at 30 min and on). This radical and complex reorganization of the actin system can also be seen in unperturbed freshly plated cells, suggesting that the actin cytoskeleton and the associated adhesions are highly dynamic structures. [Ballestrem et al., 1998]. This reorganization suggests that the balance of mechanical force within cells, which is generated and regulated by different elements of the cytoskeleton, is highly dynamic, too [Ingber, 2003]. The constant change in forces acting on FA can, in turn, affect their assembly and stability. The mechanism responsible for the coordination of these complex assembly processes is still poorly understood and it remains to be determined whether they are primarily driven by an inherent instability of the actomyosin network and the associated signaling systems, which regulate its organization, or whether other cytoskeletal filaments such as microtubules play an active role in this process [Elbaum et al., 1999].

As indicated above, it is well established that the assembly of focal adhesions and the associated stress fibers depends on the application of mechanical forces to the endogenous (e.g., actomyosin contractility) or exogenous (e.g., shear stress) contact site [Bershadsky et al., 1996; Riveline et al., 2001]. Is the formation of adhesions in spreading cells also dependent upon local mechanical force? Based on preliminary experiments in which cells were allowed to undergo spreading in the presence of contractility inhibitors such as H-7, it appears that the development of adhesive structures is effectively blocked (data not shown).

The data described here highlight the mechanism involved in the development of the very first contractile bundles formed during spreading. We propose that the earliest forms of matrix adhesions detected during spreading are small dots containing vinculin, integrin, phosphotyrosine, and paxillin, with the actin core, the formation of which is either force independent or requires a relatively low tension just like focal complexes [Galbraith et al., 2002; Jiang et al., 2003]. The actin core of these dots may recruit different actin-associated proteins, including actin motors such as myosin II, which can then apply force to the surrounding “plaque.” This applied force may lead to the extension of the adhesion site along the direction of the greater force and loss of adhesion in the perpendicular direction. Recent studies indicated that the assembly of adhesion sites is regulated by applied mechanical forces, suggesting that it contains a “mechanosensor” that translates tension into an assembly signal [Geiger and Bershadsky, 2002]. Such a signal does not appear to involve activation of stress-responsive channels since protein recruitment to adhesion sites can occur in detergent-permeabilized cell models following a general stretching of the cells [Sawada and Sheetz, 2002]. Such a process might lead to an apparent “splitting” of

the vinculin/paxillin ring into a doublet structure, interconnected by actin filaments. Such primordial complexes consisting of short actin bundles, anchored at both ends in focal adhesions, can further grow and reorganize into larger and more complex structures, resembling short stress fibers. Formation of many such complexes is followed by global reorganization of the actin cytoskeleton, as described above. This reorganization appears to be driven, to a large extent, by mechanical forces too. For example, end-to-end lining up of FS-FA complexes can change the polarized stress applied to FA by the interconnecting SF such that FA that are positioned along the new, fused actin bundle (rather than at the end) may be pulled in opposite directions and the stress applied to them may thus be reduced. This may, in turn, lead to a partial or complete disassembly of these “internal” adhesions.

Apparently, this mode of assembly of integrin-bound adhesions described here is different from the mechanism observed in well-spread cells, particularly during cell migration, which is dominated by “typical” stress fibers, anchored to focal complex-derived FA that are located mainly at the cell periphery. While distinct in their fine details, the different mechanisms underlying the formation of FA-SF complexes during spreading and motility are driven by a similar mechanosensitive process, whose precise molecular nature is yet to be determined.

**ACKNOWLEDGMENTS**

We are grateful to Alexander Bershadsky and Prof. Zvi Kam for insightful comments and suggestions. We thank Dr. Joachim Kirchner for the preparation of the YFP-actin vector, and Orna Yeager and Ilana Sabanay for their help with the electron microscopy. B.G. holds the E. Neter chair for Cell and Tumor Biology.

**REFERENCES**

Ayscough K. 1998. Use of latrunculin-A, an actin monomer-binding drug. *Methods Enzymol* 298:18–25.  
 Ballestrem C, Wehrle-Haller B, Imhof A. 1998. Actin dynamics in living mammalian cells. *J Cell Sci* 111:649–6458.  
 Ballestrem C, Hinz B, Imhof B, Wehrle-Haller BA. 2001. Marching at the front and dragging behind: differential alphaVbeta3-integrin turnover regulates focal adhesion behavior. *J Cell Biol* 155:1319–1332. Epub 2001 Dec 24.  
 Bar-Ziv R, Thlusty T, Moses E, Safran SA, Bershadsky A. 1999. Pearlring in cells: a clue to understanding cell shape. *Proc Natl Acad Sci USA* 96:10140–10145.  
 Bershadsky A, Chausovsky A, Becker E, Lyubimova A, Geiger B. 1996. Involvement of microtubules in the control of adhesion-dependent signal transduction. *Curr Biol* 6:1279–1289.  
 Burridge KM, Chrzanowska-Wodnicka M. 1996. Focal adhesions, contractility, and signaling. *Annu Rev Cell Dev Biol* 12:463–518.  
 Cramer LP, Siebert M, Mitchison TJ. 1997. Identification of novel graded polarity actin filament bundles in locomoting heart fibroblasts: implications for the generation of motile force. *J Cell Biol* 136:1287–1305.

Elbaum M, Chausovsky A, Levy ET, Shtutman M, Bershadsky A. 1999. Microtubule involvement in regulating cell contractility and adhesion-dependent signalling: a possible mechanism for polarization of cell motility. *Biochem Soc Symp* 65:147–72.  
 Galbraith CG, Yamada KM, Sheetz MP. 2002. The relationship between force and focal complex development. *J Cell Biol* 159:695–705.  
 Geiger B, Bershadsky A. 2001. Assembly and mechanosensory function of focal contacts. *Curr Opin Cell Biol* 13:584–592.  
 Geiger B, Bershadsky A. 2002. Exploring the neighborhood. Adhesion-coupled cell mechanosensors. *Cell* 110:139–142.  
 Geiger B, Bershadsky A, Pankov R, Yamada KM. 2001. Transmembrane crosstalk between the extracellular matrix and the cytoskeleton. *Nat Rev Mol Cell Biol* 2:793–805.  
 Geiger B. 1979. A 130K protein from chicken gizzard: its localization at the termini of microfilament bundles in cultured chicken cells. *Cell* 18(1):193–205.  
 Helfman DM, Levy ET, Berthier C, Shtutman M, Riveline D, Grosheva I, Lachish-Zalait A, Elbaum M, Bershadsky AD. 1999. Cadesmon inhibits nonmuscle cell contractility and interferes with the formation of focal adhesions. *Mol Biol Cell* 10:3093–3112.  
 Ingber DE. 2003. Tensegrity I. Cell structure and hierarchical systems biology. *J Cell Sci* 116:1157–1173.  
 Jiang G, Giannone G, Critchley DR, Fukumoto E, Sheetz MP. 2003. Two-piconewton slip bond between fibronectin and the cytoskeleton depends on talin. *Nature* 424:334–337.  
 Leopoldt D, Yee HF, Rozengurt E Jr. 2001. Calyculin-A induces focal adhesion assembly and tyrosine phosphorylation of p125(Fak), p130(Cas), and paxillin in Swiss 3T3 cells. *J Cell Physiol* 188:106–119.  
 Linder S, Aepfelbacher M. 2003. Podosomes: adhesion hot-spots of invasive cells. *Trends Cell Biol* 13:376–385.  
 Machesky L, Hall MA. 1997. Role of actin polymerization and adhesion to extracellular matrix in Rac- and Rho-induced cytoskeletal reorganization. *J Cell Biol* 138:913–926.  
 Neff NT, Lowrey C, Decker C, Tovar A, Damsky C, Buck C, Horwitz AF. 1982. A monoclonal antibody detaches embryonic skeletal muscle from extracellular matrices. *J Cell Biol* 95:654–666.  
 Nobes C, Hall DA. 1995. Rho, rac, and cdc42 GTPases regulate the assembly of multimolecular focal complexes associated with actin stress fibers, lamellipodia, and filopodia. *Cell* 81:53–62.  
 Riveline D, Zamir E, Balaban NQ, Schwarz US, Ishizaki T, Narumiya S, Kam Z, Geiger B, Bershadsky AD. 2001. Focal contacts as mechanosensors: externally applied local mechanical force induces growth of focal contacts by an mDia1-dependent and ROCK-independent mechanism. *J Cell Biol* 153:1175–1186.  
 Rottner K, Hall A, Small JV. 1999. Interplay between Rac and Rho in the control of substrate contact dynamics. *Curr Biol* 9:640–648.  
 Sawada Y, Sheetz MP. 2002. Force transduction by Triton cytoskeletons. *J Cell Biol* 156:609–615.  
 Schoenwaelder S, Burridge MK. 1999. Bidirectional signaling between the cytoskeleton and integrins. *Curr Opin Cell Biol* 11:274–286.  
 Small JV, Rottner K, Kaverina I, Anderson KI. 1998. Assembling an actin cytoskeleton for cell attachment and movement. *Biochim Biophys Acta* 1404:271–281.  
 Tian B, Millar C, Kaufman PL, Bershadsky A, Becker E, Geiger B. 1998. Effects of H-7 on the iris and ciliary muscle in monkeys. *Arch Ophthalmol* 116:1070–1077.  
 Volberg T, Geiger B, Citi S, Bershadsky AD. 1994. Effect of protein kinase inhibitor H-7 on the contractility, integrity, and membrane anchorage of the microfilament system. *Cell Motil Cytoskeleton* 29:321–338.  
 Zamir E, Geiger B. 2001. Molecular complexity and dynamics of cell-matrix adhesions. *J Cell Sci* 114:3583–3590.  
 Zamir E, Katz BZ, Aota S, Yamada KM, Geiger B, Kam Z. 1999. Molecular diversity of cell-matrix adhesions. *J Cell Sci* 112:1655–1669.